Journal of Applied Polymer Science

# Hybrid Clay-Carbon Nanotube/PET Composites: Preparation, Processing, and Analysis of Physical Properties

**Giuliana Gorrasi,[1] Salvatore D'Ambrosio,[2] Giovanni Patimo,[2] Roberto Pantani[1]**
[1]Department of Industrial Engineering, University of Salerno, Via Giovanni Paolo II 132, 84084 Fisciano, Salerno, Italy
[2]Department of Physics, University of Salerno, Via Giovanni Paolo II 132, 84084 Fisciano, Salerno, Italy
Correspondence to: G. Gorrasi (E-mail: ggorrasi@unisa.it)

**ABSTRACT:** The aim of this work was the preparation of novel composites of poly(ethylene terephthalate) (PET) and nano-hybrid systems based on clay used as catalyst for the growth of multi walled carbon nanotubes (Clay-CNTs), through catalytic chemical vapor deposition (CCVD). The carbon content into the hybrid filler was 58.1 wt %. Composites with 1.0, 1.5, 2.0, 3.0 wt % of Clay–CNTs were obtained by melt compounding and processed using a microinjection molding press. Unfilled PET was processed in the same composites conditions. Structural characterization and physical properties (thermal, degradation, mechanical, and electrical) were analyzed and correlated to the hybrid filler loading, and carbon nanotubes amount. © 2014 Wiley Periodicals, Inc. J. Appl. Polym. Sci. **2014**, *131*, 40441.

**KEYWORDS:** composites; polyesters; molding

Received 25 October 2013; accepted 11 January 2014
**DOI: 10.1002/app.40441**

## INTRODUCTION

Poly(ethylene terephthalate) (PET) is one of the most widely used thermoplastic polyesters in the world.[1] In the last few decades the applications of PET expanded in a variety of fields, ranging from fibers to soft drink bottles to films and magnetic recording tape substrates.[2,3] Although PET possesses balanced properties of mechanical strength, thermal property, and barrier property for commodity and engineering applications, the further improvement in thermal and mechanical properties of this polymer is needed to pursue higher performance applications. Nanocomposite technology has been proved to be an effective way to improve physical properties of polymers by using several nanofillers, such as carbon nanotubes,[4–8] graphene,[9–11] clay,[12–15] silica,[16–18] etc. Furthermore, it is well known that the microstructure of polymeric manufactures is the result of the parameters imposed during the processing conditions.[19–21] The complex thermo-mechanical history experienced by a polymer during processing results in a large anisotropy of the final physical properties, particularly if the polymer is semicrystalline and is filled with particles of large aspect ratio. The increasingly rapid rise of miniaturized parts and the rapid development of microsystem technologies have opened up new applications for polymer nanocomposites. Microinjection molding is one of the most suitable processing for producing microparts cheaply and with high precision. As for the conventional injection molding, the physical properties of manufactures made by microinjection molding are strongly affected by the processing parameters. However, because of the characteristics of microinjection molding, these parameters and their effects are function of the materials processed (i.e., polymer, type of filler, amount of filler, degree of filler dispersion).

Catalytic chemical vapor deposition (CCVD) or hot filament chemical vapor deposition are the prevailing synthetic methods and acetylene, methane or ethylene are used as carbon sources. Montmorillonite,[22–25] clinoptilolite,[25] laponite[24] added with first-row transition metals from Cr to Zn are used as catalysts. Among the added metals, Fe, Co, Ni and Mn are the most suitable for the growth of MWCNT by CCVD of acetylene at 700°C,[22–24] whereas Cu mainly leads to the formation of C nanospheres and Cr, Zn are not active at all.[23]

Very recently a novel nano-material, obtained by direct catalytic chemical vapor deposition (CCVD) growth of carbon nanotubes (CNTs) (CNT content into the hybrid: 58.1 wt %) over a clay mineral catalyst, was incorporated into Polylactic acid (PLA). Thermal, mechanical, barrier and UV resistance were improved.[26,27] In this article we used a PET matrix as host of such nano-hybrid filler. The nano-hybrid (here named Clay-CNTs) was incorporated into PET using a twin screw extruder, at different filler percentage (1.0, 1.5, 2.0, and 3.0 wt %). Such compositions were chosen in order to ensure a well balanced presence of inorganic clay and carbon nanotubes, aimed at the

improvement of the different explored physical properties. Pure PET was submitted to the same thermomechanical history. PET and nano-composites were submitted to micro-molding. Morphological organization and physical properties (thermal, mechanical, electrical) were analyzed and correlated to the filler content. The world wide application of PET stimulated this study using hybrid filler, in order to investigate the possibility to apply it in new technological fields.

## EXPERIMENTAL

### Materials

The Poly(ethylene terephthalate) (PET) adopted in this work is produced by M&G Polimeri Italia S.p.A with the commercial trade name of CLEARTUF P76 (intrinsic viscosity is 0.74 dL $g^{-1}$). The nano-hybrid filler used was obtained according to a previously reported procedure.[26] Clay mineral-carbon nanotube was synthesized by direct growth of CNT by CCVD on sodium exchanged muscovite catalysts (Sigma–Aldrich, Italy). Iron catalyst was prepared by wet impregnation of $Na^+$-exchanged clay mineral. After drying at 80°C, the catalyst was calcined at 450°C in air and reduced for 2 h under hydrogen flow (60 $cm^3$ $min^{-1}$) at 500°C. The CCVD synthesis was carried out at 700°C in the presence of i-$C_4H_{10}$ and $H_2$. Nearly 0.5 g of reduced catalyst was placed in a quartz boat inside the quartz reactor, located in a horizontal electric furnace, and preliminarily heated up to synthesis temperature under 120 $cm^3$ $min^{-1}$ 1:1 He-$H_2$ flow. It was then replaced with i-$C_4H_{10}$ keeping a constant flow ratio and total flow rate. i-$C_4H_{10}$ represents the carbon source. The reaction was stopped after 2 h and the raw products were subsequently cooled down to room temperature in He atmosphere. The weight percentage of C deposited was calculated as C (wt %) = $100 \cdot (m - m_{0R})/m$, where $m$ is the mass of all the materials (reaction products and catalyst) after synthesis and $m_{0R}$ is the mass of the catalyst after reduction. CCVD of isobutane on the clay catalysts led to nano-hybrid containing 58.1 wt % of deposited carbon. After cooling, support and iron particles were removed by refluxing the composites obtained in a mixture of 12% HCl and 12% HF acids. Finally, C deposits were washed thoroughly with distilled water and dried at 110°C for 3 h.

### Composite Preparation

The composites were obtained by melt compounding adopting a twin screw counter-rotating intermeshing mixer (Haake Minilab II) which allows for recycling in order to improve the dispersion and distribution of the filler within the polymer. The well dried polymer and a weigthed amount of filler were starve-fed until a complete filling of the mixer was reached. Several attempts were carried out in order to select the optimal mixing conditions: the screw rotation speed was kept as high as possible with the aim of achieving an optimal dispersion of the filler; the temperature was selected as the lowest possible, compatible with the maximum torque of the mixer, to minimize the thermal degradation of the polymer; the recycling time was chosen as the minimum which allowed to obtain a homogeneous material, without visible agglomerates. The mixing conditions are summarized in Table I. Several composites were prepared containing different weight percent of Clay-CNTs: 1.0, 1.5, 2.0, and 3.0%. For comparison, also the pure PET was processed following the same procedure as the composites. Immediately after compounding, the composites were injection molded by adopting a HAAKE MiniJet in a rectangular mold 60-mm long, 10-mm wide, and 500-$\mu$m thick. The molding conditions are summarized in Table II. It is worth noticing that it was possible to injection mold the compounds at lower temperature and pressures with respect to pure PET. Indeed, with the same conditions adopted for the pure PET, flash occurred: the material came out from the cavity passing through the gap between the two halves of the mold. This phenomenon compelled to reduce both injection and mold temperature to injection mold the filled materials. On the other hand, injection molding tests conducted with the pure PET adopting the same conditions defined for the filled materials resulted in incomplete moldings. It was therefore evident that the compounds presented a better fluidity. This can be due either to a reduction of elongational viscosity or to an additional lowering of the molecular weight induced by the presence of the fillers.

**Table I.** Processing Parameters Applied During Compounding

| | |
|---|---|
| Temperature | 280°C |
| Screws rotation speed | 200 rpm |
| Recycling time | 4 min |
| Fed mass | 7 g |

### Methods

X-ray diffraction measurements (XRD) were performed with a Brucker diffractometer (equipped with a continuous scan attachment and a proportional counter) with Ni-filtered Cu K$\alpha$ radiation ($\lambda = 1.54050$ Å).

Thermogravimetric analysis (TGA) was carried out with a Mettler TC-10 thermobalance. The samples were heated from 25 to 1000°C at 10°C $min^{-1}$ heating rate under air flow. The weight loss was recorded as function of temperature.

Differential scanning calorimetry (DSC) analysis was carried out on samples with a mass ranging between 10 and 12 mg. The tests were carried out by means of a DTA Mettler Toledo (DSC 30) under nitrogen atmosphere. The samples were heated from 25 to 280°C at 10°C $min^{-1}$, cooled from 280 to 25°C at 10°C $min^{-1}$, and reheated from 25 to 280°C at 10°C $min^{-1}$.

Mechanical properties were evaluated using a DMA TAQ800. Measurements were conducted at the constant frequency (1 Hz)

**Table II.** Processing Parameters Applied During Injection Molding

| | PET | PET + filler |
|---|---|---|
| Injection temperature | 300°C | 280°C |
| Mold temperature | 70°C | 50°C |
| Injection pressure | 250 bar | 100 bar |
| Injection time | 2 s | 1 s |

and amplitude (5 μm). The temperature was varied between 0 and 120°C at 3°C $min^{-1}$.

The electrical conductivity was measured at room temperature with a Keithley 6517A electrometer unit in a two-probe resistance measurement configuration controlled by a computer. The source delay for each point of measurement was about 3 s. For each measurement, the sample was placed between two copper electrodes. To enhance the electrical contact between the samples and the electrodes, metallization with Au was used. The metallization was conducted using a Agar Auto Sputter Coater (Agar Scientific Limited, UK). The metallization time was 180 s, for a metal deposition of about 22 nm. The electrical conductivity was measured in the voltage range −10 to 10 V. The electrical conductivity, $\sigma$ (S $cm^{-1}$), of all the samples was obtained by using the basic equation[24]:

$$\sigma = \frac{L}{dW}\frac{1}{R} = \frac{L}{dW}\frac{I_{measured}}{V_{applied}} \quad (1)$$

where $R(\Omega) = V_{applied}/I_{measured}$, $d$ (m), $W$ (m), and $L$ (m) are the resistance, the thickness, the width and the length of the specimens respectively. Data averaged on three specimens.

## RESULTS AND DISCUSSIONS

### WAXD Analysis

Figure 1 reports the X-ray diffractograms evaluated on the PET, Clay–CNTs filler and composites at different nano-hybrid concentration. PET does not show any crystallinity evidence, the pattern is amorphous with the maximum of the hallow at $2\theta \approx 21.2°$. The composites present a peak at about 25.8° of $2\theta$, that is due to the filler diffraction.[26] PET in presence of the filler tends to mainly retain its amorphous structure at all compositions.

### DSC Analysis

The thermograms obtained during the first heating scan of the molded samples made of pure PET and of all the compounds are reported in Figure 2. The results of calorimetric analysis are reported in Table III. It is possible to notice that the glass transition temperature of the compounds is lower with respect to the pure PET (about 5°C). This can be interpreted with a higher mobility of the amorphous phase induced by the filler.

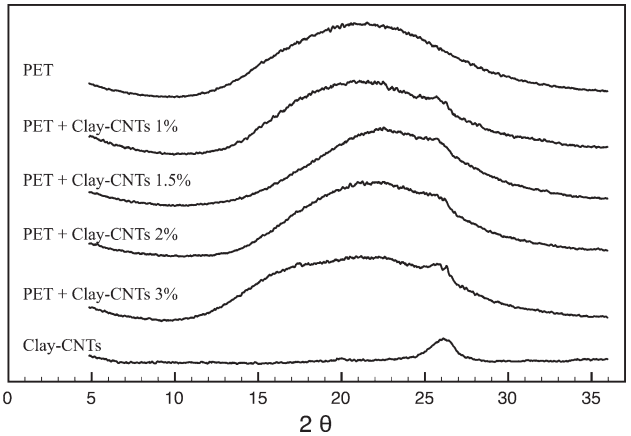


**Figure 1.** WAXD of PET, clay–CNTs filler and composites.

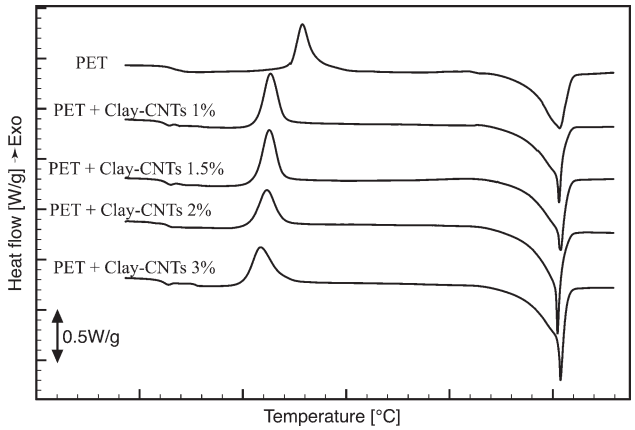


**Figure 2.** First heating run of PET and composites with different clay–CNTs fillers.

The amount of filler does not seem to affect the glass transition temperature. It is also possible to notice that cold crystallization takes place at lower temperatures (105–110°C) for compounds with respect to pure PET (125°C). An increase of the filler content induces a lower temperature of colder crystallization (namely a faster crystallization kinetics). This could be due to a larger number of nuclei induced by the filler. The increase of crystallization kinetics is confirmed by the thermograms obtained during the cooling scan (Figure 3). The crystallization temperature increases of about 25°C, from about 200°C for pure PET to more than 225°C for the compounds. From the thermograms obtained during the second heating scan (Figure 4) it is possible to notice that the melting temperature of the pure PET and of the compounds is the same: the presence of filler does not affect the crystal perfection and thus their melting.

### Thermogravimetric (TGA) Analysis

Thermal stability of PET and its composites under air conditions was investigated using a thermo-gravimetric analyzer. TGA curves of pure PET and the composites with different Clay-CNTs content are shown in Figure 5. The degradation of pure PET and nano-composite can be divided into two steps. The first step is attributed to the decomposition of initial materials, and the second step is due to the consumption of char under the air atmosphere.[28] Typical thermo-oxidative degradation temperatures for 5, 50, and 90% of weight loss under the air gases condition are also summarized in Table IV. The substantial enhancement in the thermal stability of PET/Clay-CNTs nanohybrids can be attributed to the barrier effect of clay sheets dispersed into the PET matrix, respect to the volatile decomposed products, as well as the air gases permeating through the composites. In addition, the presence of CNTs may hinder the thermo-oxidation of PET entrapping free radicals produced during the thermo-oxidation process.[29,30]

### Mechanical Properties

Figure 6 reports he storage modulus G′ measured during heating of pure PET moulded, and samples filled with 1.0 and 3.0 wt % of Clay-CNTs. It can be noticed that an increase of the modulus is reached. In particular, the modulus increases on

**Table III.** Calorimetric Data on PET and Composites Evaluated from Plots 2, 3, and 4

| | 1st heating scan | | | | | Cooling scan | | 2nd heating scan | |
|---|---|---|---|---|---|---|---|---|---|
| Sample | $T_g$ (°C) | $\Delta H_c$ (W g$^{-1}$ pol$^{-1}$) | $T_c$ (°C) | $\Delta H_m$ (W g$^{-1}$ pol$^{-1}$) | $T_m$ (°C) | $\Delta H_c$ (W g$^{-1}$ pol$^{-1}$) | $T_c$ (°C) | $\Delta H_m$ (W g$^{-1}$ pol$^{-1}$) | $T_m$ (°C) |
| PET | 68 | 27.7 | 129 | −49.1 | 253 | 44.0 | 194 | −42.4 | 250 |
| PET + Clay-CNTs 1.0% | 63 | 27.8 | 113 | −46.3 | 253 | 44.9 | 222 | −52.7 | 250 |
| PET + Clay-CNTs 1.5% | 63 | 33.0 | 113 | −50.6 | 254 | 41.3 | 224 | −52.9 | 250 |
| PET + Clay-CNTs 2.0% | 65 | 23.8 | 112 | −52.1 | 252 | 49.6 | 224 | −57.7 | 250 |
| PET + Clay-CNTs 3.0% | 62 | 27.1 | 109 | −52.1 | 253 | 42.2 | 226 | −51.9 | 250 |

increasing the percentage of Clay-CNTs in the composite. This is due mainly to the reinforcing effect of clay lamellae. The increase is particularly relevant at high temperatures: at 50°C the modulus increases of a factor 2 for 1% of Clay-CNTs and of a factor 2.5 for 3% of Clay-CNTs. The increase of modulus for all the samples taking place at 60°C can be also due to a release of orientation in the molded samples taking place close to the glass transition temperature.[31]

### Electrical Properties

The electrical conductivity of the different PET/CNT-Clay nano-hybrids, was measured in the voltage range −10÷10 V. From the I–V measurements, the contact geometry and the measured sample thickness, the electrical conductivity, $\sigma$ (S cm$^{-1}$) has been determined. Being the carbon nanotubes the conducting nanoparticles, the current flow and the percolation threshold is attributed to their presence and degree of dispersion. Figure 7 shows the electrical conductivity, $\sigma$ (S cm$^{-1}$), as function on CNTs (wt %) into the composites. PET matrix shows an insulating behavior with an electrical conductivity around $1 \times 10^{-17}$ S cm$^{-1}$.[32,33] It is evident that already at 1.0 wt % of nano-hybrid (i.e., 0.581 wt % of CNTs) the electrical conductivity increases of about eight orders of magnitude. With increasing CNTs content the conductivity slightly increases reaching a plateau value for about 1.0 wt % of CNTs. According to the traditional percolation theory,[34] the electrical conductivity of electro-conductive composite materials can be predicted by the following equation:

$$\sigma_{comp} = \sigma_0 (x - x_c)^{\tau} \text{ for } x > x_c \quad (2)$$

where $\tau$ is the critical exponent, $x$ (wt %) is the weight fraction of filler, $x_c$ (wt %) is the percolation threshold, and $\sigma_0$ (S cm$^{-1}$) is a parameter basically depending on the electrical conductivity of filler. Usually, $x_c$ (wt %), $\tau$ and $\sigma_0$ (S cm$^{-1}$) can be determined experimentally fitting the experimental data from Figure 7. Using eq. (1) the best fitted values of $x_c$ (wt %), $\tau$ and $\sigma_0$ (S cm$^{-1}$) can be obtained (Figure 8). The percolation threshold results to be equal to 0.33 wt %. The value of $\sigma_0$ (S cm$^{-1}$) and $\tau$ are $3.9 \times 10^{-9}$ S cm$^{-1}$ and 0.63, respectively. The $\sigma_0$ is much lower than the expected conductivity for nanotube mats.[35] This might be due to the morphology of the composites where conductive nanotubes are growth on clay lamellae that are dielectric particles and separated by regions of insulating matrix. Hence, conduction is limited by tunnelling between potential barriers within conductive regions.[36,37] As already demonstrated,[38] such an improvement of electrical performances with the low percolation threshold could be attributed to the synergic effect of the CNTs and clay platelets. The latter favor the CNTs dispersion into the PET matrix, preventing any reagglomeration of the nanotubes during the processing (either mixing or microinjection moulding). As a result, the well dispersed CNTs could create a physical network that enhances contact resistance on areas where nanotubes are in contact each other, justifying the higher measured electrical conductivity. Figure 9 reports the relative conductivity, defined as the ratio of conductivity of the

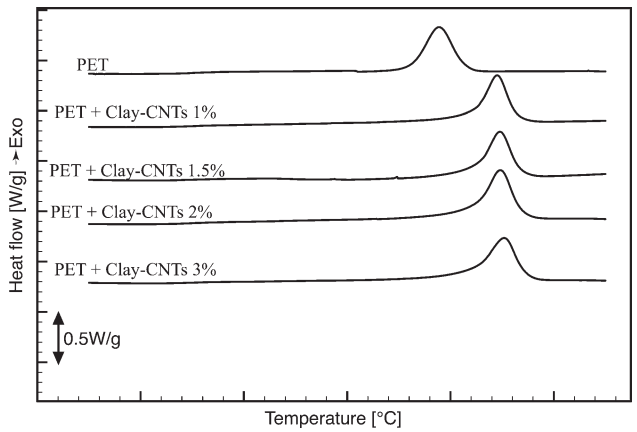


**Figure 3.** Cooling of PET and composites with different clay–CNTs filler.

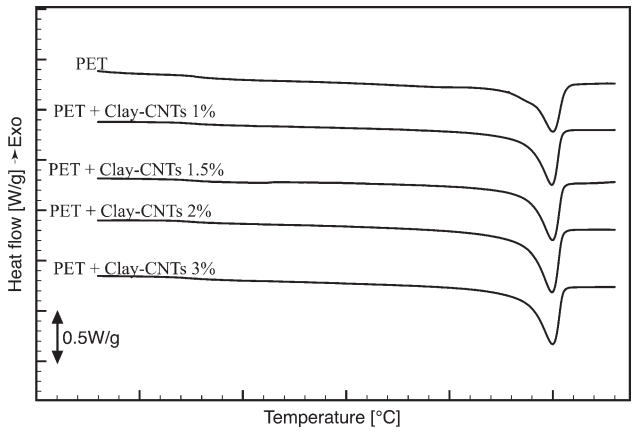


**Figure 4.** Second heating run of PET and composites with different clay–CNTs filler.

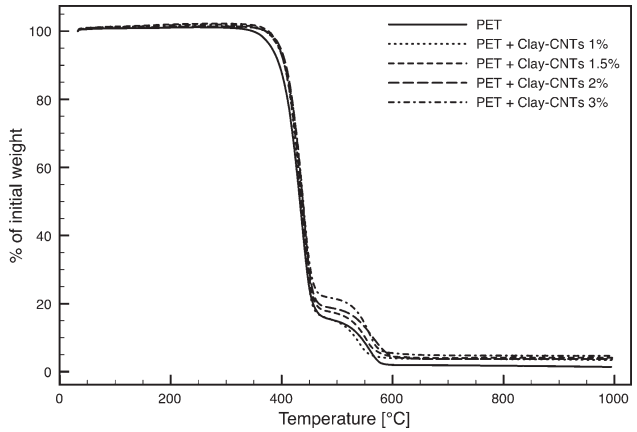


**Figure 5.** TGA curves of PET and composites with different clay–CNTs filler.

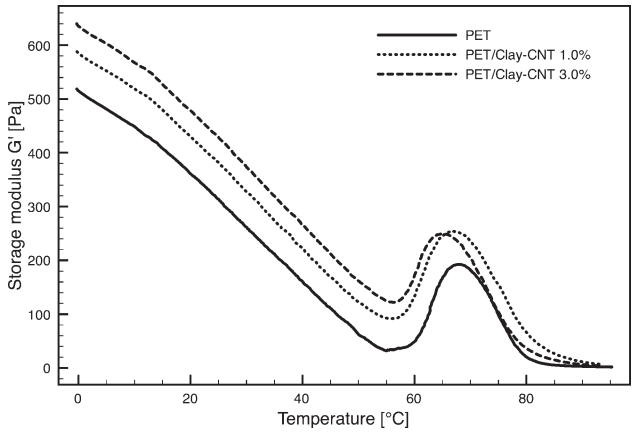


**Figure 6.** DMA curves of PET and composites with 1.0 and 3.0 wt % of clay–CNTs filler.

composite sample and conductivity of the unfilled matrix ($\sigma_{composites}/\sigma_{PET}$) in function of the nanotubes loading. The relative conductivity increases linearly on a semi-log plot. This is true relatively to the composition range investigated in the present work. The fitting equations are reported on the graph. It is useful for a good prediction of the electrical conductivity for such nano-compositions at any filler loading[39,40]

## CONCLUDING REMARKS

Novel composites based on Poly(ethylene terephthalate) (PET) and a nano-hybrid filler based on clay used as catalyst for the growth of multi walled carbon nanotubes (Clay-CNTs), were prepared by melt compounding and processed using a microinjection molding. The multi walled nanotube content into the filler was 58.1 wt %. The filler content was 1.0, 1.5, 2.0, 3.0 wt %. Structural characterization and analysis of physical properties was carried out and correlated to the hybrid filler loading, and carbon nanotubes amount.

- X-ray analysis showed that with the used processing conditions PET and composites had a morphological organization with PET chains in the amorphous state. The composite loaded with 3.0 wt % of Clay-CNTs filler presented a not fully amorphous morphology. The filler, at this content, acted as nucleating agent on the polymer.

**Table IV.** Degradation Temperatures Evaluated from TGA Plots for PET and Composites

| Sample | $T_{(5\%\ wt\ loss)}$ | $T_{(50\%\ wt\ loss)}$ | $T_{(90\%\ wt\ loss)}$ |
|---|---|---|---|
| PET | 382°C | 433°C | 543°C |
| PET+Clay-CNTs 1.0% | 395°C | 435°C | 538°C |
| PET+Clay-CNTs 1.5 % | 396°C | 437°C | 552°C |
| PET+Clay-CNTs 2.0% | 398°C | 438°C | 565°C |
| PET+Clay-CNTs 3.0% | 395°C | 440°C | 562°C |

- Differential scanning calorimetric analysis showed that the cold crystallization for composites took place at lower temperatures with respect to pure PET. This could be due to a larger number of nuclei induced by the filler.
- Thermogravimetric analysis showed a substantial enhancement in the thermal stability of PET/Clay-CNTs nanohybrids. It has been attributed to the barrier effect of clay sheets dispersed into the PET matrix to the volatile low molecular weight products. Furthermore, the presence of CNTs may hinder the thermo-oxidation of PET entrapping free radicals produced during the thermal scan.
- Elastic modulus, evaluated through dynamic mechanical analysis, showed an improvement with filler loading. Such an improvement is mainly due to the clay platelets that act as reinforcing agent.
- Electrical conductivity was evaluated as function of CNTs content. It was demonstrated that already at 0.581 wt % of CNTs the electrical conductivity increased of about eight orders of magnitude. With increasing CNTs content the conductivity slightly incremented reaching a plateau value for about 1.0 wt % of CNTs. The percolation threshold was found to be 0.33 wt % of CNTs. Such result was attributed to the clay platelets that favored the CNTs dispersion into the

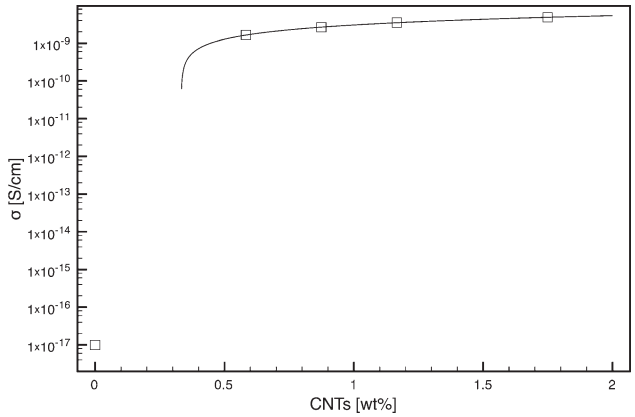


**Figure 7.** Electrical conductivity, $\sigma$ (S $cm^{-1}$), as function of CNTs (wt %) into the composites.

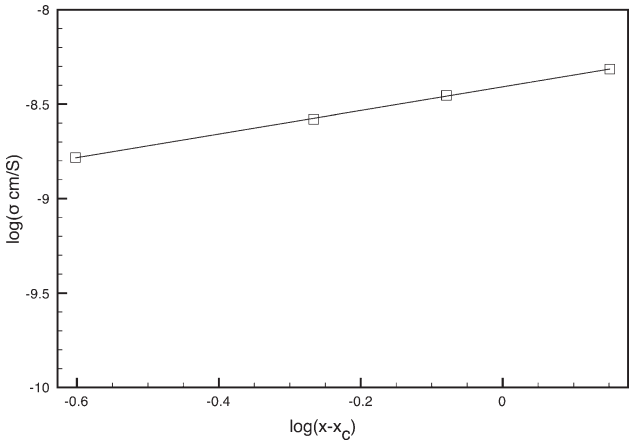


**Figure 8.** Log of $\sigma$ (S cm$^{-1}$), ad function of Log of difference between $x$ (weight fraction of filler in wt %) and $x_c$ (percolation threshold in wt %).

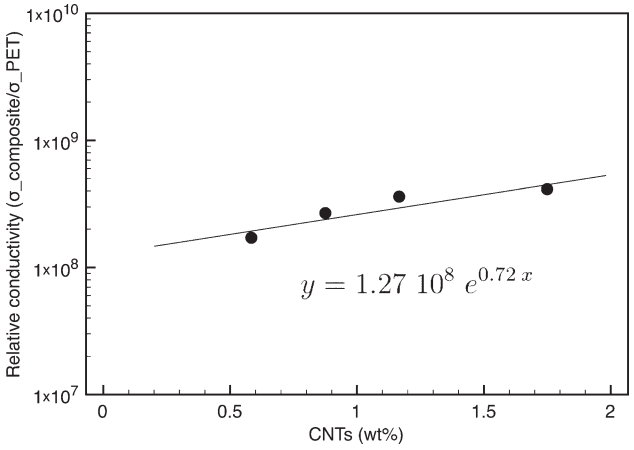


**Figure 9.** Relative conductivity ($\sigma_{composites}/\sigma_{PET}$) as function of CNTs (wt %) into the composites.

PET matrix, preventing any reagglomeration of the nanotubes during the processing. The resulted physical network, with enhanced contact between conductive nanotubes, was responsible for the improvement of electrical conductivity and low percolation threshold.

## REFERENCES


1. John, S.; Long, T. E., Eds. Modern Polyesters: Chemistry and Technology of Polyesters and Copolyesters; Wiley, Chichester, England **2003**.
2. Mark, H. F.; Kroschwitz, J. I. Encyclopedia of Polymer Science and Engineering; Wiley: New York, **1985**.
3. Bhimaraj, P.; Burris, D. L.; Action, J.; Sawyer, W. G.; Toney, C. G.; Siegel, R. W.; Schadler, L. S. *Wear* **2005**;*258*:1437.
4. Sandler, J. K. W.; Kirk, J. E.; Kinloch, I. A.; Shaffer, M. S. P.; Windle, A. H. *Polymer* **2003**, *44*, 5893.
5. Potschke, P.; Abdel-Goad, M.; Alig, I.; Dudkin, S.; Lellinger, D. *Polymer* **2004**, *45*, 8863.
6. Lee, H. J.; Oh, S. J.; Choi, J. Y.; Kim, J. W.; Han, J.; Tan, L. S.; Baek, J. B. *Chem. Mater.* **2005**, *17*, 5057.
7. Yoon, J. T.; Jeong, Y. G.; Lee, S. C.; Min, B. G. *Polym. Adv. Technol.* **2009**, *20*, 631.
8. Gomez-del Rio, T.; Poza, P.; Rodriguez, J.; Garcia-Gutierrez, M. C.; Hernandez, J. J.; Ezquerra, T. A. *Compos. Sci. Technol.* **2010**, *70*, 284.
9. Stankovich, S.; Dikin, D. A.; Dommett, G. H. B.; Kohlhaas, K. M.; Zimney, E. J.; Stach, E. A.; Piner, R. D.; Nguyen, S. T.; Ruoff, R. S. *Nature* **2006**, *442*, 282.
10. Xiao, M.; Sun, L. Y.; Liu, J. J.; Li, Y.; Gong, K. C. *Polymer* **2002**, *43*, 2245.
11. Ramanathan, T.; Abdala, A. A.; Stankovich, S.; Dikin, D. A.; Herrera-Alonso, M.; Piner, R. D.; Adamson, D. H.; Schniepp, H. C.; Chen, X.; Ruoff, R. S.; Nguyen, S. T.; Aksay, I. A.; Prud'homme, R. K.; Brinson, L. C. *Nat. Nanotechnol.* **2008**, *3*, 327.
12. Giannelis, E. P. *Adv. Mater.* **1996**, *8*, 29.
13. Liu, X. H.; Wu, Q. *J. Polymer* **2001**, *42*, 10013.
14. Paul, D. R.; Robeson, L. M. *Polymer* **2008**, *49*, 3187.
15. Hwang, S. Y.; Lee, W. D.; Lim, J. S.; Park, K. H.; Im, S. S. *J. Polym. Sci. B Polym. Phys.* **2008**, *46*, 1022.
16. Ou, Y. C.; Yang, F.; Yu, Z. Z. *J. Polym. Sci. B Polym. Phys.* **1998**, *36*, 789.
17. Ji, Q.; Wang, X. L.; Zhang, Y. H.; Kong, Q. S.; Xia, Y. Z. *Compos. A Appl. Sci. Manufact.* **2009**, *40*, 878.
18. Munstedt, H.; Koppl, T.; Triebel, C. *Polymer* **2010**, *51*, 185.
19. Pantani, R.; Coccorullo, I.; Speranza, V.; Titomanlio, G. *Prog. Polym. Sci.* **2005**, *30*, 1185.
20. Pantani, R.; Coccorullo, I.; Speranza, V.; Titomanlio, G. *Polymer* **2007**, *48*, 2778.
21. Pantani, R.; Sorrentino, A.; Speranza, V.; Titomanlio, G. *Indus. Eng. Chem. Res.* **2012**, *51*, 10840.
22. Gournis, D.; Karakassides, M. A.; Bakas, T.; Boukos, N.; Petridis, D. *Carbon* **2002**, *40*, 2641.
23. Bakandritsos, A.; Simopoulos, A.; Petridis, D. *Chem. Mater.* **2005**, *17*, 3468.
24. Tsoufis, T.; Jankovic, L.; Gournis, D.; Trikalitis, P. N.; Bakas, T. *Mater. Sci. Eng. B Adv. Funct. Solid State Mater.* **2008**, *152*, 44.
25. Kadlecikova, M.; Breza, J.; Jesenak, K.; Pastorkova, K.; Luptakova, V.; Kolmacka, M.; Vojackova, A.; Michalka, M.; Vavra, I.; Krizanova, Z. *Appl. Surf. Sci.* **2008**, *254*, 5073.
26. Santangelo, S.; Gorrasi, G.; Di Lieto, R.; De Pasquale, S.; Patimo, G.; Piperopoulos, E.; Lanza, M.; Faggio, G.; Mauriello, F.; Messina, G.; Milone, C. *Appl. Clay Sci.* **2011**, *53*, 188.
27. Gorrasi, G.; Milone, C.; Piperopoulos, E.; Lanza, M.; Sorrentino, A. *Appl. Clay Sci.* **2013**, *71*, 49.
28. ASTM. Standard Test Method for Resistivity of Electrical Conductor Materials, B 193-95; Annual Book of ASTM Standards, ASTM, 1995.
29. Martin-Gullon, I.; Esperanza, M.; Font, R. *J. Anal. Appl. Pyrolysis* **2001**, *58*, 635.
30. Levchik, S. V.; Weil, E. D. *Polym. Adv. Technol.* **2004**, *15*, 691.
31. Li, M. L.; Jeong, Y. G. *Compos. A Appl. Sci. Manufact.* **2011**, *42*, 560.

32. Pantani, R.; Sorrentino, A.; Speranza, V.; Titomanlio, G. *Rheol. Acta* **2004**, *43*, 109.
33. Hu, G. J.; Zhao, C. G.; Zhang, S. M.; Yang, M. S.; Wang, Z. G. *Polymer* **2006**, *47*, 480.
34. Paszkiewicz, S.; Szymczyk, A.; Spitalsky, Z.; Soccio, M.; Mosnacek, J.; Ezquerra, T. A.; Roslaniec, Z. *J. Polym. Sci. Part B: Polym. Phys.* **2012**, *50*, 1645.
35. Deutsher, G. In Percolation, Localization, and Superconductivity; Goldman, A. M., Wolf, S. A., Eds.; Plenum Press: New York, **1984**.
36. Chen, Q.; Wang, S.; Peng, L. M. *Nanotechnology* **2006**, *17*, 1087.
37. Inam, F.; Peijs, T. *Adv. Compos. Lett.* **2006**, *15*, 7.
38. Deng, H.; Skipa, T.; Zhang, R.; Lellinger, D.; Bilotti, E.; Alig, I.; Peijs, T. *Polymer* **2009**, *50*, 3747.
39. Gorrasi, G.; Piperopoulos, E.; Lanza, M.; Milone, C. *J. Phys. Chem. Solids* **2013**, *74*, 1.
40. Gorrasi, G.; Bredeau, S.; Di Candia, C.; Patimo, G.; De Pasquale, S.; Dubois, P. *Macromol. Mater. Eng.* **2011**, *296*, 408.